Inorganic Chemistry

Article

pubs.acs.org/IC

Combined Time-Resolved Laser Fluorescence Spectroscopy and Extended X-ray Absorption Fine Structure Spectroscopy Study on the Complexation of Trivalent Actinides with Chloride at T = 25−200 °C

Andrej Skerencak-Frech,*[,†] Daniel R. Fröhlich,[†,‡] Jörg Rothe,[†] Kathy Dardenne,[†] and Petra J. Panak[‡]

[†]Institut für Nukleare Entsorgung, Karlsruher Institut für Technologie (KIT)—Campus Nord, D-76344, Eggenstein-Leopoldshafen, Germany

[‡]Physkalisch-Chemisches Institut, Ruprecht Karls Universität Heidelberg, D-69120 Heidelberg, Germany

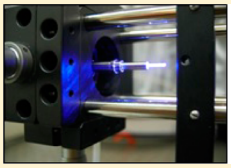

$$Cm^{3+} + n\,Cl^- \rightleftharpoons CmCl_n^{3-n}$$

$$TRLFS + SIT, EXAFS$$
$$T = 25 - 200°C$$

$$\log K_n^0(T), \varepsilon_{i,k}(T)$$
$$\Delta_r H_m^0, \Delta_r S_m^0, \Delta_r C_{p,m}^0$$
$$Structure\ data$$

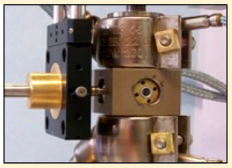

ABSTRACT: The complexation of trivalent actinides (An(III)) with chloride is studied in the temperature range from 25 to 200 °C by spectroscopic methods. Time-resolved laser fluorescence spectroscopy (TRLFS) is applied to determine the thermodynamic data of Cm(III)−Cl^- complexes, while extended X-ray absorption fine structure spectroscopy (EXAFS) is used to determine the structural data of the respective Am(III) complexes. The experiments are performed in a custom-built high-temperature cell which is modified for the respective spectroscopic technique. The TRLFS results show that at 25 °C the speciation is dominated mainly by the Cm^{3+} aquo ion. Only a minor fraction of the $CmCl^{2+}$ complex is present in solution. As the temperature increases, the fraction of this species decreases further. Simultaneously, the fraction of the $CmCl_2^+$ complex increases strongly with the temperature. Also, the $CmCl_3$ complex is formed to a minor extent at T > 160 °C. The conditional stability constant log β'_2 is determined as a function of the temperature and extrapolated to zero ionic strength with the specific ion interaction theory approach. The log $\beta^\circ_2(T)$ values increase by more than 3 orders of magnitude in the studied temperature range. The temperature dependency of log β°_2 is fitted by the extended van't Hoff equation to determine $\Delta_r H^\circ_m$, $\Delta_r S^\circ_m$, and $\Delta_r C^\circ_{p,m}$. The EXAFS results support these findings. The results confirm the absence of americium(III) chloride complexes at T = 25 and 90 °C ([Am(III)] = 10^{-3} m, [Cl^-] = 3.0 m), and the spectra are described by 9−10 oxygen atoms at a distance of 2.44−2.48 Å. At T = 200 °C two chloride ligands are present in the inner coordination sphere of Am(III) at a distance of 2.78 Å.

1. INTRODUCTION

Since 1954 nuclear fission has been used for the peaceful generation of electrical power. However, the safe disposal of the accumulating nuclear waste is still an unsolved problem. Due to neutron capture reactions within the reactor, the waste contains plutonium as well as minor actinides (e.g., neptunium, americium, and curium). Some of these nuclides have very long half-lives (e.g., $t_{1/2}(^{239}Pu)$ = 2.4 × 10^4 years). Thus, the disposal of the nuclear waste requires an isolation from the biosphere over very long time scales (>10^5 years). In general, a repository in a deep geological formation is considered as the best option for the disposal of the waste. A comprehensive long-term safety assessment of such a repository should be based on a reliable thermodynamic description of the geochemical processes relevant for the migration or retention of the actinides. Considerable effort was invested in the past to establish a thermodynamic database for the actinides in their most relevant oxidation states.[1,2] However, the majority of the available data are valid only for ambient temperatures. Due to the radioactive decay of the nuclear waste, the temperature in the near field of a repository may reach up to 200 °C. Up to now, only little information has been available on the temperature dependency of the chemistry and thermodynamics of the actinides under geochemical conditions. A detailed review of literature data up to 90 °C is given by Rao.[3] However, very few data are available at T > 100 °C. This lack of information makes the prediction of the temperature effect on the migration behavior of the actinides a difficult task. Therefore, additional thermodynamic data are required not only at room temperature but also at increased temperatures.

Furthermore, detailed thermodynamic data at increased temperatures are of importance for aquatic chemistry in general. For example, hydrothermal saline solutions play an important role in the field of ocean chemistry, e.g., in the vicinity of black and white smokers. A detailed understanding of the chemical processes in these hydrothermal saline solutions is of high scientific interest to explain the origins of life.[4,5] Furthermore, aquatic solutions at high temperatures and pressure are also found in various geochemical systems. For

Received: October 9, 2013
Published: January 2, 2014

   dx.doi.org/10.1021/ic4025603 | *Inorg. Chem.* 2014, 53, 1062−1069

example, the migration of rare-earth elements in hydrothermal solutions in ore deposits plays an important role during a variety of geological processes. Only limited data are available on the extent and mechanism of this transport.

Chloride is present in large quantities in the brines of deep salt formations as well as in the pore water of certain clay rocks. At ambient temperatures, Cl^- is a weak ligand for the complexation of trivalent actinides.[1] Furthermore, literature data on the complexation of An(III) with Cl^- are divided into two groups. The majority of the available data have been determined by two-phase equilibrium methods (e.g., ion exchange and liquid−liquid extraction). The other group of data are based on spectroscopic techniques. The stability constants determined by spectroscopic methods are about 2 orders of magnitude lower. This discrepancy is explained by the inability of the methods based on a two-phase equilibrium to distinguish between ion−ion interaction (outer-sphere complexes) and the formation of inner-sphere complexes. Especially in the case of very weak ligands such as Cl^-, the replacement of large amounts of the background electrolyte by high concentrations of the ligand causes changes in the activity coefficients which are misinterpreted as complex formation. This effect leads to a large scattering of the available log β_n data.

Fanghänel et al. and Könnecke et al. used the Pitzer equation to derive a quantitative model for the formation of $AnCl_n^{(3-n)+}$ complexes at 25 °C over a wide concentration range (log $\beta^\circ_1(25\ ^\circ C)(AnCl^{2+}) = 0.24 \pm 0.03$ and log $\beta^\circ_2(25\ ^\circ C)(AnCl_2^{+}) = -0.74 \pm 0.05$).[6,7] These values were selected by the Nuclear Energy Agency Thermochemical Database (NEA-TDB) project as the best estimate for the equilibrium constants of chloride complexes with trivalent actinides at ambient temperatures.[1]

Literature data on the complexation of trivalent actinides with chloride at increased temperatures are scarce. Yeh et al. used a solvent extraction method to study the formation of $AmCl^{2+}$ complexes in 1.0 M $NaClO_4$ at T = 25 and 50 °C.[8] The authors determined a slight increase of log $\beta'_1(25\ ^\circ C)(AmCl^{2+}) = 0.11 \pm 0.05$ to log $\beta'_1(50\ ^\circ C)(AmCl^{2+}) = 0.38 \pm 0.05$ in the studied temperature range, yielding a reaction enthalpy of $\Delta_r H = 19.39 \pm 7.35$ kJ/mol. In contrast to this, Choppin et al. and Moulin et al. determined small negative values for the standard reaction enthalpy ($\Delta_r H \approx -0.21$ kJ/mol).[9,10] However, no ionic strength corrections were made by the authors. For trivalent lanthanides more literature data on the complexation with Cl^- at elevated temperatures is available, especially at $T >$ 100 °C. Further details are given in section 3.1.3. In general, a strong increase of the log β°_n values (n = 1, 2) by several orders of magnitude with the temperature was determined.

In the present study, we apply advanced spectroscopic techniques (time-resolved laser fluorescence spectroscopy (TRLFS) and extended X-ray absorption fine structure spectroscopy (EXAFS)) in combination with a custom-built high-temperature cell to study the formation of $AnCl_n^{(3-n)+}$ (An = Cm, Am) complexes at T = 25−200 °C. Cm(III) (for TRLFS) and Am(III) (for EXAFS) are chosen as representatives for trivalent actinides in the present work to determine the thermodynamic data (log β°_n, $\Delta_r H^\circ_m$, $\Delta_r S^\circ_m$, $\Delta_r C^\circ_{p,m}$) and structural parameters of $AnCl_n^{(3-n)+}$ complexes at increased temperatures. Since the chemical properties of f-elements are mainly defined by their oxidation state, the behaviors of Cm(III) and Am(III) will be similar under the present experimental conditions.

2. EXPERIMENTAL SECTION

All concentrations are given on the molal concentration scale (mol/kg of H_2O, m) to avoid a temperature-dependent deviation of the concentration.

2.1. TRLFS. A Cm(III) stock solution ($[Cm(III)] = 2.12 \times 10^{-5}$ m) with an isotopic composition of 89.7% ^{248}Cm, 9.4% ^{246}Cm, 0.3% ^{244}Cm, and 0.6% ^{243}Cm, ^{245}Cm, and ^{247}Cm is used. With this, the total Cm(III) concentration in the TRLFS samples is set to 10^{-7} m. The proton concentration in every sample is fixed at 8.926×10^{-2} m with HCl. The chloride concentration is set to 0.505, 1.008, 2.021, 2.519, 3.034, 3.501, and 4.003 m by adding solid NaCl. The measurements are performed in a custom-built high-temperature cell. Details on the technical setup are given elsewhere.[11] For the TRLFS measurements, the laser beam is coupled to the cell by a customized optical waveguide. This waveguide consists of a central quartz fiber surrounded by an additional bundle of eight smaller fibers. The single center fiber is used for the transmission of the laser beam into the cell. The resulting fluorescence light is collected by the eight outer fibers and transmitted to the detector system.

An excimer-pumped dye laser system (Lamba Physics EMG 201 and FL 3002) with a pulse energy of about 2−4 mJ at a repetition rate of 10 Hz is used for excitation. The spectra are recorded by an optical multichannel analyzer, consisting of a polychromator (Jobin Yvon HR320) with a 1200 line/mm grating (Andor Technology, SR3-GRT-1200-500, blaze 500 nm, resolution 0.21 nm) and a time-gateable intensified photodiode array with 1024 Si photodiodes (Spectroscopy Instruments ST 180, IRY700 9).

The peak deconvolution of the experimental emission spectra is performed with the software OriginPro (OriginLab Corp., v8.5.0 SR1). The ratios of the single-component spectra are varied until their sum fits the experimental spectrum. The quality of the fit is reflected by the residue (difference between the sum of single-component spectra and the experimental spectrum).

2.2. EXAFS. The EXAFS sample is prepared by adding 304 μL of an Am(III) stock solution ($[^{243}Am] = 30$ MBq/L, $[^{241}Am] = 17$ MBq/L) to 5 mL of a chloride stock solution, resulting in a total Am(III) concentration of 10^{-3} m. The Cl^- concentration of the chloride stock solution is set to 3.0 m by adding solid NaCl. The proton concentration is adjusted to 8.926×10^{-2} m with HCl. For EXAFS measurements the high-temperature cell described in ref 11 is modified. The modified cell is displayed in Figure 1.

Two of the quartz windows are replaced by windows made of metallic beryllium and coated with Kapton tape (see Figure 1). Be shows a permeability of 92% for photons with an energy of 17.6 keV, enabling EXAFS studies at the Am L_{III}-edge (18.5 keV). All EXAFS measurements are performed at the INE-Beamline of the Angström-quelle Karlsruhe (ANKA, Karlsruhe, Germany).[12] The beamline is equipped with a double-crystal monochromator (DCM) and a collimating and focusing mirror system (Rh-coated silicon mirrors). In the present study, a Ge(422) crystal pair is used in the DCM. The DCM is detuned in the middle of the scan range to 70% peak flux intensity. The spectra are collected in fluorescence mode at an angle of 90° using a five-pixel Ge detector (Canberra Ultra-LEGe). The incident X-ray intensity I_0 is measured with an Ar-filled ionization chamber at ambient pressure. Within the EXAFS range, the measurement is performed at equidistant k-steps and the integration time is increased continuously with a $\sqrt{2}$ progression. Measurements are performed at T = 25, 90, and 200 °C. The data are evaluated with the software packages EXAFSPAK, Athena 0.8.061, and Artemis 0.8.012.[13−15] Theoretical scattering phases and amplitudes are calculated with FEFF8.40 using the crystal structures of AmO_2 (for samples showing no chloride) or AmOCl.[16,17] In all cases, the models are fitted to the k^3-weighted raw EXAFS spectra.

3. RESULTS AND DISCUSSION

3.1. TRLFS. *3.1.1. Emission Spectra.* The emission spectra at T = 25−200 °C and $[Cl^-] = 2.02$ m are displayed in Figure 2a. A pronounced decrease of the emission intensity by about

dx.doi.org/10.1021/ic4025603 | Inorg. Chem. 2014, 53, 1062−1069

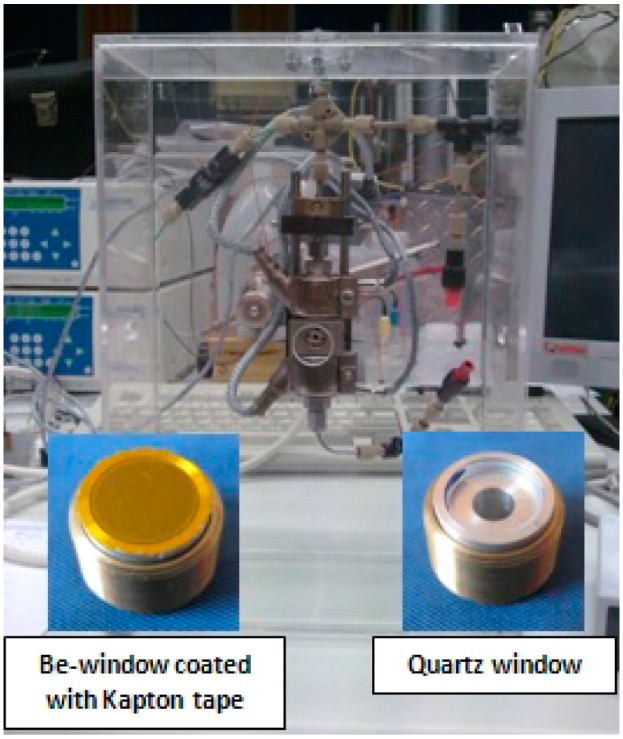

Figure 1. High-temperature cell for EXAFS together with the applied windows (quartz and Be, coated with Kapton tape).

50% is observed as the temperature increases to 200 °C. This temperature-dependent loss of emission intensity is comparable to observations described in the literature for the curium(III) sulfate system.[18] The reason for this effect is still under discussion. Tian et al. showed that up to 100 °C a thermal population of higher energetic levels of the Cm(III) ion and successive nonradiative deexcitation explain this loss of emission intensity.[19] However, at T > 100 °C additional quenching mechanisms have to be considered.[11,18] Also, sorption effects to the cuvette walls are enhanced at higher temperatures. For better comparison and further evaluation, the spectra are normalized to equal peak areas (Figure 2b). The spectra are shifted distinctively toward higher wavelengths with increasing temperature. This effect results from a larger splitting of the $^6D'_{7/2}$ state of the Cm(III) ion and may originate from two different reactions. On one hand, the equilibrium between 9- and 8-fold-hydrated Cm(III) species is shifted toward the latter as the temperature increases.[20] On the other hand, the formation of inner-sphere $CmCl_n^{(3-n)+}$ complexes also leads to a shift of the emission band to higher wavelengths. To differentiate between these two effects, the spectra of Cm(III) in aqueous NaCl and $NaClO_4$ are compared. Perchlorate is a very weak ligand toward trivalent actinides and does not form complexes with Cm(III) at $[ClO_4^-]$ < 7.0 m and $T \leq$ 200 °C.[20] Thus, the spectra obtained in perchlorate solutions represent the Cm(III) aquo ion at the respective temperature, and differences in spectra obtained in chloride media must originate from the formation of different $CmCl_n^{(3-n)+}$ species. The spectra recorded at two different ionic strengths and T = 25, 100, and 200 °C are displayed in Figure 3.

At 25 °C only marginal differences in the emission spectra in NaCl and $NaClO_4$ are observable. These originate from an additional minor emission band at 594.5 nm, which is attributed to a small fraction of the $CmCl^{2+}$ complex.[6,21] This is in good agreement with the literature. According to the data given by the NEA-TDB project, the $CmCl^{2+}$ complex is formed as a minor species (<5%) at $[Cl^-]$ < 6 m.[1] As the temperature increases, the emission spectra in NaCl solutions are shifted distinctively further toward higher wavelengths compared to the $NaClO_4$ solutions. This indicates a significant increase of the molar fractions of the $CmCl_n^{(3-n)+}$ (n > 1) complexes.

3.1.2. Peak Deconvolution and Speciation. To determine the molar fractions of the different curium(III) chloride complexes, the single-component spectra of the respective species as a function of the temperature are required. They are determined from the experimental emission spectra at different temperatures. The peak positions of the emission bands are in excellent agreement with literature data for the $CmCl_n^{(3-n)+}$ complexes (594.9 nm (n = 1), 598.3 nm (n = 2), 605.0 nm (n = 3)).[6,21] At 25 °C, the intensity of the emission band of the $CmCl^{2+}$ complex is very low and almost disappears with increasing temperature. Thus, the emission band is determined at T < 100 °C and with a low signal-to-noise ratio. The $CmCl_3$ complex is formed at $T \geq$ 160 °C. The respective spectrum determined under these conditions also shows a high signal-to-noise ratio. The single-component spectra of the $CmCl_2^+$ complex are determined in good quality at T = 50−200 °C. Two examples of peak-deconvoluted emission spectra ($[Cl^-]$ = 1.01 m, T = 25 °C; $[Cl^-]$ = 4.01 m, T = 200 °C) are displayed in Figure 4.

To derive the species concentrations from the peak areas of the single components, the quantum yields of the individual curium(III) chloride species have to be considered. The

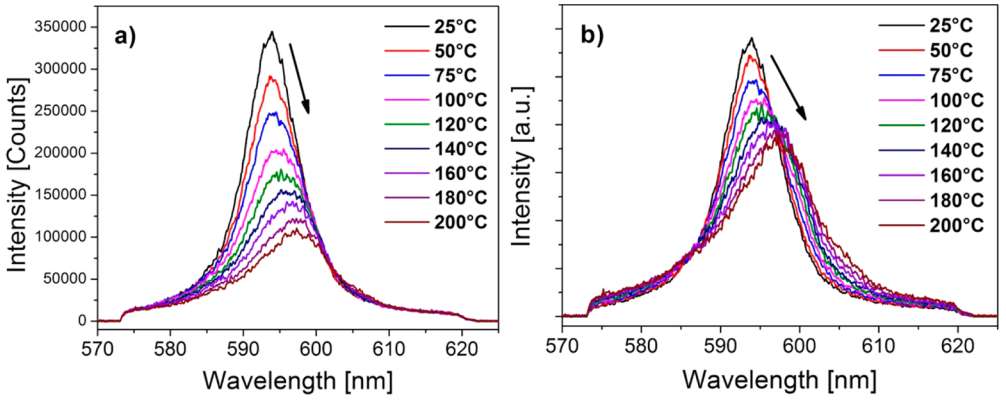

Figure 2. Emission spectra of Cm(III) in aqueous NaCl solution at T = 25−200 °C ($[NaCl]$ = 2.02 m, $[H^+]$ = 8.93 × 10^{-2} m).

dx.doi.org/10.1021/ic4025603 | Inorg. Chem. 2014, 53, 1062−1069

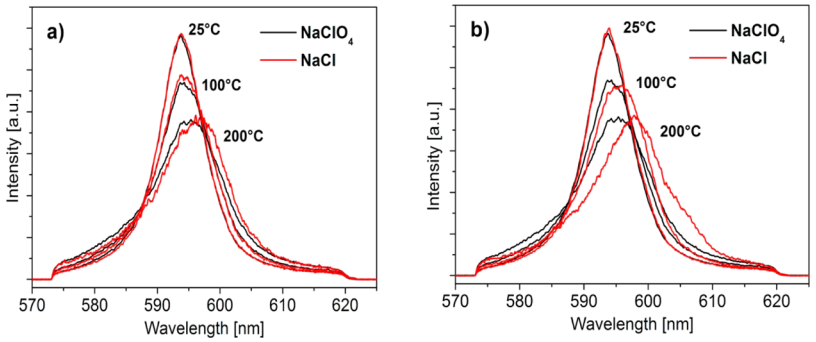

Figure 3. Comparison of the emission spectra of Cm(III) in aqueous NaCl and $NaClO_4$ at T = 25, 100, and 200 °C: (a) $[Cl^-]$ = 0.505 *m*, $[ClO_4^-]$ = 0.505 *m*, (b) $[Cl^-]$ = 4.003 *m*, $[ClO_4^-]$ = 4.003 *m*.

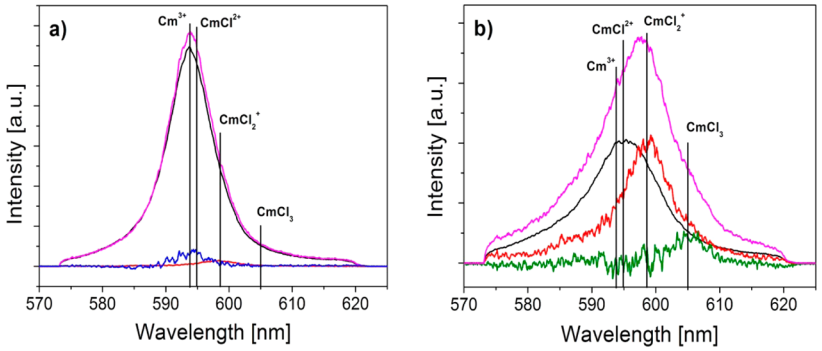

Figure 4. Single-component spectra of the $CmCl_n^{(3-n)+}$ complexes (n = 1, 2, 3) and two examples of peak-deconvoluted emission spectra of Cm(III) at (a) $[Cl^-]$ = 1.01 *m* and T = 25 °C and (b) $[Cl^-]$ = 4.01 *m* and T = 200 °C.

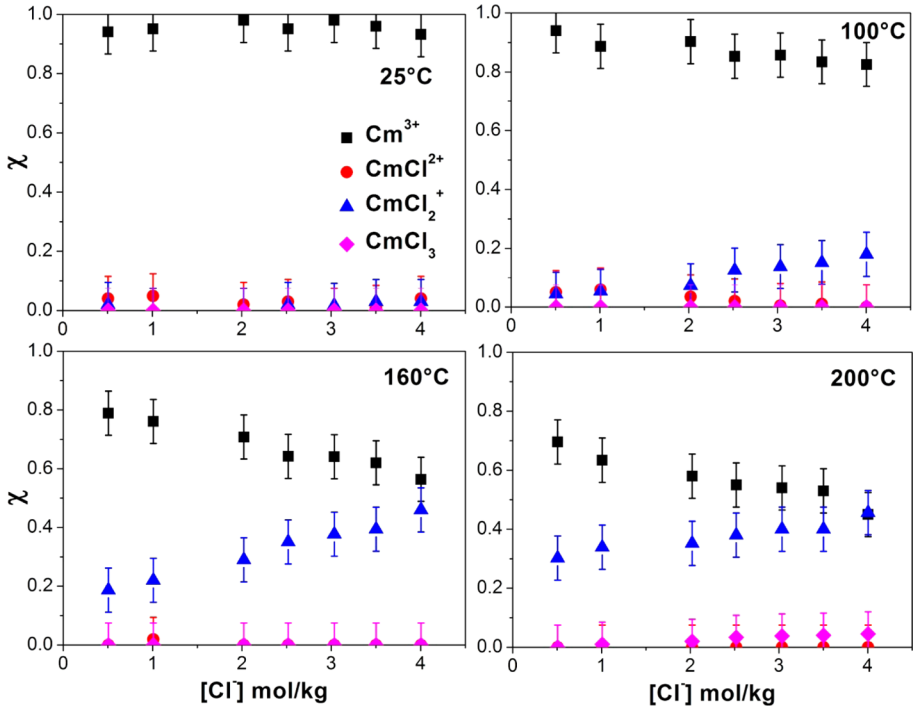

Figure 5. Molar fractions of the $CmCl_n^{(3-n)+}$ complexes (n = 0, 1, 2, 3) as a function of $[Cl^-]$ at T = 25, 100, 160, and 200 °C.

quantum yield of a complex is accounted for by its fluorescence intensity factor (FI factor). Fanghänel et al. showed that at 25 °C the FI factors of the individual $CmCl_n^{(3-n)+}$ (n = 0, 1, 2, 3) species are almost identical.[6] Furthermore, the decay of the fluorescence emission is in accordance with a monoexponential decay law at each studied chloride concentration and temperature. This is typical for systems where the exchange of the ligands is considerably faster compared to the fluorescence lifetime of the complexed species. Thus, the species distribution is governed by the thermodynamic equilibrium, and differences in the FI factors of the $CmCl_n^{(3-n)+}$ species would influence solely the overall emission intensity and

dx.doi.org/10.1021/ic4025603 | Inorg. Chem. 2014, 53, 1062−1069

not their relative intensity ratios. Further details on this topic are given elsewhere.[22]

Therefore, the FI factors of the different curium(III) chloride species are treated as unity, and their molar fractions are derived directly from the relative emission intensity of the respective bands. Species distributions as a function of $[Cl^-]$ and at T = 25, 100, 160, and 200 °C are displayed in Figure 5.

The given error of ±0.05 of the molar fraction is a conservative estimation of all uncertainties which may accumulate throughout the data treatment, mainly resulting from the peak deconvolution procedure. At room temperature, very small amounts (<5%) of curium(III) chloride complexes are present and the speciation is dominated by the Cm^{3+} aquo ion. No higher complexes are formed in the studied Cl^- concentration range. The speciation changes considerably at higher temperatures. The fraction of the Cm^{3+} aquo ion decreases with increasing chloride concentration. No increase of the $CmCl^{2+}$ complex is observed. However, due to the small shift of the emission band of the $CmCl^{2+}$ complex compared to Cm^{3+} (∼ 1 nm) and the red shift of the emission bands due to the increased formation of 8-fold-coordinated species at increased temperatures (see section 3.1.1), the determination of this species at T > 50 °C is difficult and accompanied by a rather large error. For further information see section 3.1.3. The fraction of the $CmCl_2^+$ complex increases significantly at higher temperatures. For example, at 200 °C the concentration of $CmCl_2^+$ is equal to that of the Cm^{3+} aquo ion. At $T \geq$ 160 °C the $CmCl_3$ complex starts to form, yet remains below 5%. Due to the low signal-to-noise ratio of the spectra of the $CmCl^{2+}$ and $CmCl_3$ complexes, the respective molar fractions are estimations and should be treated with caution. Additionally, the determined speciation at each temperature is governed by two effects. On one hand, the increase of the ligand concentration results in the formation of $CmCl_n^{(3-n)+}$ species, according to the law of mass action. On the other hand, the increase of the chloride concentration is also accompanied by a considerable change of the activities of the reactive species. These changes may be misinterpreted as complex formation. To distinguish between these two effects, the respective activity coefficients have to be considered in the thermodynamic description of the americium(III) chloride system.

3.1.3. Thermodynamics. Due to the low molar fractions of the $CmCl^{2+}$ and $CmCl_3$ complexes, the conditional stability constants of these species ($\log \beta'_1$, $\log \beta'_3$) cannot be determined with acceptable accuracy in a chloride concentration range up to 4 *m*. In contrast to that, the molar fraction of the $CmCl_2^+$ complex increases considerably with the temperature, and the $\log \beta'_2(T)$ values are determined at T = 50 − 200 °C according to

$$\beta'_2 = \frac{[Cm(Cl)_2^+]}{[Cm^{3+}][Cl^-]^2} \quad (1)$$

For the following considerations, two assumptions have to be made: First, NaCl is completely dissociated under the present experimental conditions. Second, HCl is not formed up to 200 °C. This approach is valid, since the pK° values of HCl and NaCl are well below 1 at T < 200 °C.[23,24] Thus, the total chloride concentration equals the free ligand concentration under the present conditions. As mentioned above, the conditional $\log \beta'_2(T)$ values are dependent on the activity coefficients. As an example, the $\log \beta'_2$ values at 200 °C are displayed as a function of $[Cl^-]$ in Figure 6 (squares).

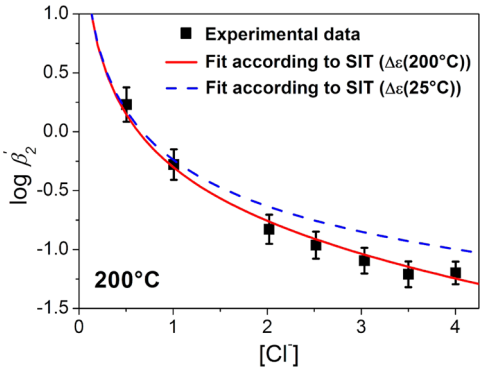

Figure 6. $\log \beta'_2$ values as a function of $[Cl^-]$ at T = 200 °C.

To compare these data with the literature, the stability constants have to be extrapolated to a standard state. In general, this is the theoretical state of infinite dilution (I_m = 0). The NEA-TDB project recommends the less parametrized SIT (specific ion interaction theory) approach over the Pitzer equation for ionic strength corrections of thermodynamic data at increased temperature.[1] The SIT is valid for $I_m \leq$ 4.0. Therefore, the chloride concentration is limited to 4.0 *m* in the present work. According to the SIT, the thermodynamic stability constants $\log \beta^\circ_n(T)$ are related to the conditional stability constants $\log \beta'_n(T)$ according to

$$\log \beta^\circ_n(T) = \log \beta'_n(T) - \Delta(z^2)\, D(T) + \Delta\varepsilon_n(T) I_m \quad (2)$$

with $\Delta(z^2) = -10$ for n = 2 and $\Delta\varepsilon_n = \sum\varepsilon_{products} - \sum\varepsilon_{educts}$. $D = (A(T)I_m^{0.5})/(1 + Ba_j(T)I_m^{0.5})$ is the Debye–Hückel term, with A and B being temperature-dependent parameters and a_j an ion size parameter. By the use of a data set of $\log \beta'_n$ at different ionic strengths, $\log \beta^\circ_n$ is derived by plotting $\log \beta'_n - \Delta(z^2)D$ versus I_m and linear regression analysis. The y-axis intercept at x = 0 corresponds to $\log \beta^\circ_n$ and the slope to $-\Delta\varepsilon_n$. The thermodynamic $\log \beta^\circ_2(T)$ values are given in Table 1.

Table 1. $\log \beta^\circ_2(T)$ Values for the Formation of the $CmCl_2^+$ Complex

T (°C)	$\log \beta^\circ_2$	T (°C)	$\log \beta^\circ_2$	T (°C)	$\log \beta^\circ_2$
25	−0.81 ± 0.35[a]	100	1.09 ± 0.13	160	2.17 ± 0.11
50	0.00 ± 0.25	120	1.48 ± 0.15	180	2.45 ± 0.10
75	0.62 ± 0.21	140	1.82 ± 0.14	200	2.83 ± 0.09

[a]Value calculated from the thermodynamic data given in Table 2.

At 25 °C the fraction of the $CmCl_2^+$ complex is too low to determine the stability constant. Thus, the $\log \beta^\circ_2$(25 °C) value given in Table 1 is calculated from the $\Delta_r H^\circ_m$ and $\Delta_r S^\circ_m$ values (see Table 2). The result is in excellent agreement with the value given by the NEA-TDB project ($\log \beta^\circ_2$(25 °C) = −0.74 ± 0.03).[1]

Literature data on the complexation of trivalent actinides with chloride at T > 25 °C are scarce. Yeh et al. studied the complexation of Am(III) with Cl^- in 1.0 M $NaClO_4$ at T = 25–50 °C.[8] The authors determined an increase of $\log \beta'_1$(25 °C) = 0.11 ± 0.05 to $\log \beta'_1$(50 °C) = 0.38 ± 0.05. No ionic strength corrections were made by the authors. Thus, the given data are only conditional values. No literature data for $\log \beta^\circ_2$ of trivalent actinides with Cl^- exist at increased temperatures. However, a few studies on trivalent lanthanides at $T \leq$ 200 °C

dx.doi.org/10.1021/ic4025603 | Inorg. Chem. 2014, 53, 1062–1069

are available. Gammons et al. applied solubility measurements to study the formation of $NdCl_n^{(3-n)+}$ complexes at T = 25−300 °C (n = 1, 2).[25] Ionic strength corrections were made according to an early form of the SIT equation. The authors determined an increase of log β°_2(25 °C)($NdCl_2^+$) from −0.38 ± 0.5 to +2.52 ± 0.2, which is in good agreement with the results of the present work. Stepanchikova et al. studied the complexation of Nd, Sm, and Ho with chloride in the temperature range of 100−250 °C using spectrophotometry.[26] The authors applied an extended Debye−Hückel equation for ionic strength corrections. The stability constants for $NdCl_2^+$ and $SmCl_2^+$ at 200 °C are in very good agreement with the results of the present work (log β°_2(200 °C)($NdCl_2^+$) = 2.54, log β°_2(200 °C)($SmCl_2^+$) = 2.26), whereas the value for Ho is 1 order of magnitude higher (log β°_2(200 °C)($HoCl_2^+$) = 3.83). Migdisov et al. studied the complexation of a series of Ln(III) ions with chloride at T = 25−300 °C by solubility measurements and applied an extended Debye−Hückel equation for the calculation of activity coefficients.[27] The authors determined a linear increase of log β°_2(25 °C)($EuCl_2^+$) from 0.73 to 3.29. Unfortunately, no error bars are given. Considering an approximate error of ±0.2, the values are in agreement with the results of the present work.

Regarding log β°_1, it is peculiar that the fraction of $CmCl^{2+}$ does not increase with the temperature, since literature data on the first stability constant of various lanthanide(III) chloride complexes show an increase of log β°_1 by 1−2 orders of magnitude in the temperature range of T = 25−200 °C.[25−28] An increase of 2 orders of magnitude of log β'_1 would lead to a molar fraction of $CmCl^{2+}$ of about 60% at 200 °C ([Cl^-] = 0.1−1 m). This is not in agreement with the present results, since such a high fraction of a species would be clearly observable in the emission spectra. However, the literature data on the temperature dependency of log β°_1 show a rather large scattering and should be treated with caution. For example, Wood determined an increase of log β°_1(25 °C)($EuCl^{2+}$) = 0.34 to log β°_1(200 °C)($EuCl^{2+}$) = 1.05.[29] Speciation calculations show that such a temperature dependency of log β°_1 would result in an only minor fraction (<0.1) of the monochloro complex at 200 °C, which is in very good agreement with the present work.

The temperature dependency of log β°_2 can be fitted by the integrated van't Hoff equation (see Figure 7, dashed line). However, a small deviation of the experimental data from the fit is visible at higher temperatures. A slightly improved fit is achieved by additionally accounting for a constant change of the heat capacity of reaction ($\Delta_r C^\circ_{p,m}$) according to an extended integrated van't Hoff equation:[30]

$$\log \beta^\circ_2(T) = \log \beta^\circ_2(T_0) + \frac{\Delta_r H_0(T_0)}{R \ln 10}\left(\frac{1}{T_0} - \frac{1}{T}\right) + \frac{\Delta_r C^\circ_{p,m}}{R \ln 10}\left(\frac{T_0}{T} - 1 + \ln\left(\frac{T}{T_0}\right)\right) \quad (3)$$

The fit of the experimental data according to eq 3 is displayed in Figure 7 (solid line). $\Delta_r H^\circ_m$, $\Delta_r S^\circ_m$ and $\Delta_r C^\circ_{p,m}$ are summarized in Table 2.

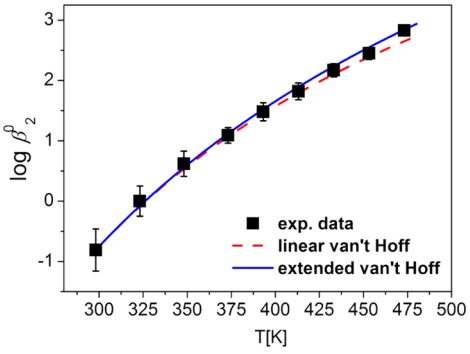

Figure 7. Fit of log $\beta^\circ_2(T)$ according to the integrated van't Hoff equation (dashed line) and extended van't Hoff equation (solid line).

Table 2. Thermodynamic Data for the Formation of the $CmCl_2^+$ Complex, $Cm^{3+} + 2Cl^- \rightleftharpoons CmCl_2^+$

$\Delta_r H^\circ_m$	54.9 ± 4.5 kJ/mol
$\Delta_r S^\circ_m$	168.8 ± 5.5 J/(mol·K)
$\Delta_r C^\circ_{p,m}$	40 ± 10 J/(mol·K)

$\Delta_r H^\circ_m$ shows a large positive value. Unfortunately, no literature data are available for comparison, yet the here-determined values are characteristic of weak ligands.[3] The standard reaction enthalpy is the sum of three different processes: First, a number of H_2O molecules are removed from the inner coordination shell of the hydrated metal ion. Second, the ligand molecule must be partially dehydrated as well. These two processes are endothermic and require energy. In the third step, the metal ion−ligand bonds are formed. This process is exothermic and thus releases energy. Due to the weak complexation strength of chloride toward trivalent actinides, only little energy is gained by the latter process, leading to largely positive standard reaction enthalpies.[31] Furthermore, a large positive $\Delta_r S^\circ_m$ is found, which originates from the release of the highly ordered water molecules from the inner coordination sphere of the Cm^{3+} aquo ion to the more disordered bulk solvent.[3] The here-determined $\Delta\varepsilon_{02}(T)$ values as a function of the temperature are displayed in Figure 8.

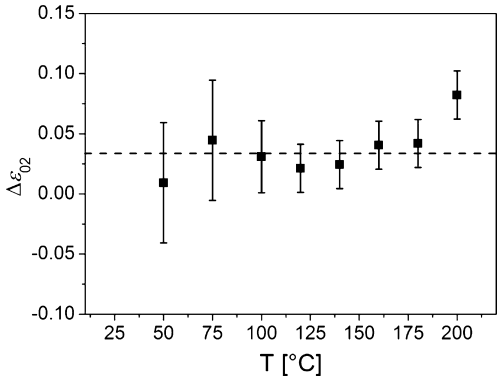

Figure 8. $\Delta\varepsilon_{02}(T)$ values for the overall formation of $CmCl_2^+$.

Due to the small fraction of the $CmCl_2^+$ complex at 25 °C, the $\Delta\varepsilon_{02}$(25 °C) value could not be determined. Up to 150 °C no temperature dependency of $\Delta\varepsilon_{02}$ is observed, resulting in a constant value of $\Delta\varepsilon_{02}$ = 0.03 ± 0.06. At higher temperatures the values increase slightly ($\Delta\varepsilon_{02}$(200 °C) = 0.08 ± 0.06). This is in very good agreement with the literature data on ion−ion interaction coefficients at T = 25−200 °C.[11,18] By using $\varepsilon(Cm^{3+},Cl^-) \approx \varepsilon(Am^{3+},Cl^-)$ = 0.23 ± 0.02 and $\varepsilon(Cl^-,Na^+)$ = 0.03 ± 0.01, a value of $\varepsilon(CmCl_2^+,Cl^-)$ = 0.32 ± 0.10 is

dx.doi.org/10.1021/ic4025603 | Inorg. Chem. 2014, 53, 1062−1069

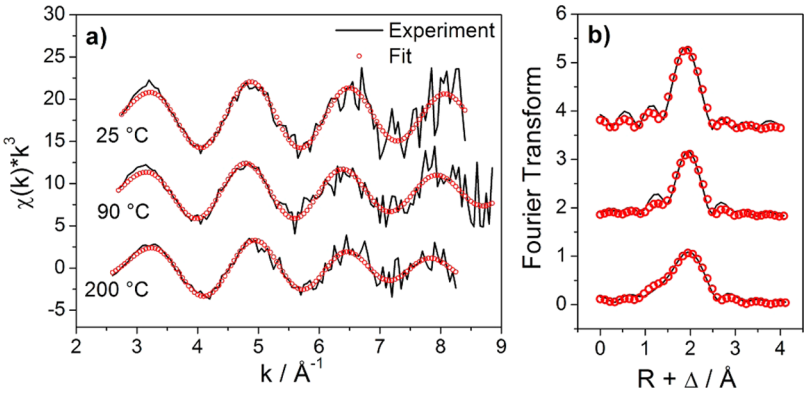

Figure 9. k^3-weighted Am L_{III}-edge EXAFS spectra (a) and related Fourier transforms (b) at T = 25, 90, and 200 °C.

determined. In Figure 6 two different fits of the ionic strength dependency of the conditional log β'_2(200 °C) values according to eq 2 are displayed. A very good fit is achieved by using the $\Delta\varepsilon_{02}$ values at 200 °C. However, application of the $\Delta\varepsilon_{02}$ values at 25 °C given by the NEA-TDB project causes only a slight deviation of the fit from the experimental data at higher ionic strengths. This confirms that the ion−ion interaction coefficients (ε) show only a minor temperature dependency, even up to 200 °C.[1,18]

3.2. EXAFS. Structural information of the formed actinide(III) chloride complexes are determined by EXAFS. The experimental background-subtracted and k^3-weighted Am L_{III}-edge EXAFS spectra as well as the corresponding Fourier Transforms are shown in Figure 9. The k-ranges for the fit of the data have been chosen individually according to the level of noise in each case.

At 25 and 90 °C the spectra are similar. At 200 °C the second oscillation at $k \approx 5$ Å^{-1} is shifted toward higher k. Consequently, the main peak in the pseudo radial distribution of the Fourier transform at $R \approx 2$ Å is broadened visibly. This effect is attributed to the presence of chloride ligands in the inner coordination sphere of the Am(III) ion. The results of the fit are displayed in Table 3.

Table 3. Structural Parameters Determined for Am(III) at [Cl⁻] = 3.0 *m* as a Function of the Temperature (Errors Given in Parentheses)[a]

T (°C)	N	R (Å)	σ^2 (Å^2)	ΔE_0 (eV)
		Am−O		
25	9.6 (2.4)	2.45 (1)	0.007 (2)	−4.9 (1.3)
90	9.0 (2.3)	2.48 (1)	0.009 (2)	−5.0 (1.3)
200[c]	6.9 (3.1)	2.34 (5)	0.017 (6)	−7.0 (3.1)
200[d]	6.3 (1.6)	2.44 (5)	0.015[b]	−5.0 (2.0)
25[e]	7.6 (0.3)	2.48	0.009[b]	−7.3
25[f]	6.4 (0.3)	2.51	0.009[b]	−6.1
		Am−Cl		
25				−4.9 (1.3)
90				−5.0 (1.3)
200[c]	2.3 (0.7)	2.69 (2)	0.005[b]	−7.0 (3.1)
200[d]	2.4 (0.6)	2.78 (4)	0.005[b]	−5.0 (2.0)
25[e]	1.2 (0.1)	2.80 (1)	0.005[b]	−7.3
25[f]	1.8 (0.1)	2.81 (1)	0.005[b]	−6.1

[a] S_0^2 = 0.9. [b] Fixed during fit. [c] Without considering a third cumulant. [d] Third cumulant set to 0.003 (Am−O) and 0.002 (Am−Cl). [e] At 10 M LiCl.[32] [f] At 12.5 M LiCl.[32]

The spectra at 25 and 90 °C are fitted by 9−10 oxygen neighbors at a distance of 2.45−2.48 Å. This is in good agreement with the literature for the Am(III) aquo ion.[32] At 200 °C 2.3 Cl^- ligands are included into the fit to describe the experimental data. Furthermore, the Debye−Waller factor of the Am−O shell increases continuously with increasing temperature from 0.007 to 0.017 Å^2. The Am−O distances obtained at T = 200 °C are significantly shorter compared to the results at 25 and 90 °C. Also, the Am−O and Am−Cl distances are significantly shorter than the literature values at T = 25 °C (see Table 3). It is known that the interatomic distance decreases with decreasing coordination number (about 0.1 Å for the change from N = 9 to N = 7).[33] However, in our case no significant change in coordination number is visible as oxygen is simply replaced by chloride, keeping the overall coordination number in the first coordination sphere constant. Therefore, the change in distance is with high certainty attributed to an asymmetric (non-Gaussian) distribution of distances which is known to occur at high temperatures.[34] To describe this effect, a third cumulant has to be included in the theoretical model. This approach yields distances for the Am−O and Am−Cl bonds of 2.44 and 2.78 Å, respectively, which are in good agreement with the literature data.[32] However, this approach does not lead to a significant improvement of the fit as the r-factors of both fits (with and without the third cumulant) stay equal at 0.078. Nevertheless, in our opinion the inclusion of this factor is essential to provide a physically appropriate result regarding the interatomic distances. In contrast to the neighbor distances, the coordination number remains constant within the range of error, whether a third cumulant is taken into account or not.

The number of coordinating chloride atoms can be compared to the TRLFS results. There, ∼0.8 ± 0.3 chloride atoms are present at the same chloride concentration and temperature. It is known that coordination numbers determined by EXAFS spectroscopy are mostly related to errors around ±1 atom. Although our final fit provided only an uncertainty of 0.7 chloride atom, this might be the most probable reason for this discrepancy.

4. SUMMARY AND CONCLUSION

In the present work a detailed spectroscopic study on the complexation of Cm(III) and Am(III) with chloride in the temperature range from 25 to 200 °C was performed. The TRLFS results show a strong increase of the fraction of the $CmCl_2^+$ complex with increasing temperature. At T > 160 °C, the $CmCl_3$ complex is also formed as a minor species. The

dx.doi.org/10.1021/ic4025603 | Inorg. Chem. 2014, 53, 1062−1069

conditional stability constant log β'_2 is determined as a function of the temperature and extrapolated to $I_m = 0$ with the SIT approach. log $\beta^\circ_2(T)$ increases by more than 3 orders of magnitude in the studied temperature range. The temperature dependency of log $\beta^\circ_2(T)$ is fitted by the extended van't Hoff equation, yielding $\Delta_r H^\circ_m$, $\Delta_r S^\circ_m$, and $\Delta_r C^\circ_{p,m}$.

In addition to the thermodynamic data, structural information on americium(III) chloride complexes is obtained by EXAFS. The structure of the $AnCl_n^{(3-n)+}$ species is studied by EXAFS spectroscopy at T = 25, 90, and 200 °C. The results show no formation of $AmCl_n^{(3-n)+}$ complexes up to 90 °C ($[Cl^-]$ = 3.0 m). However, at 200 °C approximately 2.5 chloride ligands are present in the inner coordination sphere of the Am(III) ion.

The aquatic geochemistry of trivalent actinides changes considerably at higher temperatures. Ligands which form only weak complexes with An(III) at 25 °C may be increased distinctively in their complexation strength at elevated temperatures. This effect is pronounced especially at T > 100 °C. Thus, species which are negligible under ambient conditions may play an important role in the solution speciation at T > 25 °C. Unfortunately, only very little information on the complexation reactions of An(III) under such conditions is available in the literature, making the prediction of the impact of increased temperatures on the aquatic geochemistry of actinides a difficult task. The here-determined data are of high importance for the modeling of the migration of actinides under near-field conditions and thus are valuable contributors to a comprehensive long-term safety assessment of a nuclear waste repository in deep geological formations.

AUTHOR INFORMATION

Corresponding Author

*E-mail: andrej.skerencak@kit.edu. Fax: +49 (0)721 608 23927. Phone: +49 (0)721 602 26024.

Notes

The authors declare no competing financial interest.

REFERENCES

(1) Guillaumont, R., Fanghänel, Th., Fuger, J., Grenthe, I., Neck, V., Palmer, D. A., Rand, M. H. (Nuclear Energy Agency Thermochemical Database Project, Organisation for Economic Co-operation and Development). *Chemical Thermodynamics*; Elsevier Science Publishers B.V.: Amsterdam, 2003; Vol. 5.
(2) Hummel, W., Berner, U., Curti, E., Pearson, F. J., Thoenen, T. *Nagra/PSI Chemical Thermodynamic Data Base 01/01*; Universal-Publishers: Boca Raton, FL, 2001.
(3) Rao, L. F. *Chem. Soc. Rev.* **2007**, *36*, 881.
(4) Helgeson, H. C. *Geochim. Cosmochim. Acta* **1992**, *56*, 3191.
(5) Martin, W.; Baross, J.; Kelley, D.; Russell, M. J. *Nat. Rev. Microbiol.* **2008**, *6*, 805.
(6) Fanghänel, Th.; Kim, J. I.; Klenze, R.; Kato, Y. *J. Alloys Compd.* **1995**, *225*, 308.
(7) Könnecke, T.; Fanghänel, T.; Kim, J. I. *Radiochim. Acta.* **1997**, *76*, 131.
(8) Yeh, M.; Maddison, A. P.; Clark, S. B. *J. Radioanal. Nucl. Chem.* **2000**, *243*, 645.
(9) Choppin, G. R.; Unrein, P. J. *J. Inorg. Nucl. Chem.* **1963**, *25*, 387.
(10) Moulin, N.; Hussonnois, M.; Brillard, L.; Guillaumont, F. *J. Inorg. Nucl. Chem.* **1975**, *37*, 2521.
(11) Skerencak, A.; Panak, P. J.; Hauser, W.; Neck, V.; Klenze, R.; Lindqvist-Reis, P.; Fanghänel, Th. *Radiochim. Acta* **2009**, *97*, 385.
(12) Rothe, J.; Butorin, S.; Dardenne, K.; Denecke, M. A.; Kienzler, B.; Löble, M.; Metz, V.; Seibert, A.; Steppert, M.; Vitova, T.; Walther, C.; Geckeis, H. *Rev. Sci. Instrum.* **2012**, *83*, 043105.
(13) George, G. N., Pickering, I. J. *EXAFSPAK: A Suite of Computer Programs for analysis of X-ray Absorption Spectra*; Stanford Synchrotron Radiation Laboratory: Menlo Park, CA.
(14) Ravel, B.; Newville, M. *J. Synchrotron Radiat.* **2005**, *12*, 537.
(15) Ankudinov, A. L.; Bouldin, C. E.; Rehr, J. J.; Sims, J.; Hung, H. *Phys. Rev. B* **2002**, *65*, 1.
(16) Zachariasen, W. H. *Acta Crystallogr.* **1949**, *2*, 388.
(17) Templeton, D. H.; Dauben, C. H. *J. Am. Chem. Soc.* **1953**, *75*, 4560.
(18) Skerencak, A.; Panak, P. J.; Fanghänel, Th. *Dalton Trans.* **2013**, *42*, 542.
(19) Tian, G.; Edelstein, N. M.; Rao, L. F. *J. Phys. Chem. A* **2011**, *115*, 1933.
(20) Lindqvist-Reis, P.; Klenze, R.; Schubert, G.; Fanghänel, Th. *J. Phys. Chem. B* **2005**, *109*, 3077.
(21) Arisaka, M.; Kimura, T.; Nagaishi, R.; Yoshida, Z. *J. Alloys Compd.* **2006**, *408*−*412*, 1307.
(22) Paviet, P.; Fanghänel, Th.; Klenze, R.; Kim, J. I. *Radiochim. Acta* **1996**, *74*, 99.
(23) Shock, E. L.; Oelkers, E. H.; Johnson, J. W.; Sverjensky, D. A.; Helgeson, H. C. *J. Chem. Soc., Faraday Trans.* **1992**, *88* (6), 803.
(24) Palmer, D. A., Fernandez-Prini, R., Harvey, A. H. Ionization Equilibria of Acids and Bases. *Aqueous Systems at Elevated Temperatures and Pressures*; Elsevier Science Publishers B.V.: Amsterdam, 2004.
(25) Gammons, C. H.; Wood, S. A.; Williams-Jones, A. E. *Geochim. Cosmochim. Acta* **1996**, *23*, 4615.
(26) Stepanchikova, S. A.; Kolonin, G. R. *Russ. J. Coord. Chem.* **2005**, *31*, 207.
(27) Migdisov, A. A.; Williams-Jones, A. E.; Wagner, T. *Geochim. Cosmochim. Acta* **2009**, *73*, 7087.
(28) Hass, J. R.; Shock, E. L.; Sassani, D. C. *Geochim. Cosmochim. Acta* **1995**, *59*, 4329.
(29) Wood, S. A. *Chem. Geol.* **1990**, *88*, 99.
(30) Puigdomenech, I., Rard, J. A., Plyasunov, A. V., Grenthe, I. Temperature Corrections to Thermodynamic Data and Enthalpy Calculations. In *Modelling in Aquatic Chemistry*; Grenthe, I., Puigdomenech, I., Eds.; Nuclear Energy Agency, Organisation for Economic Co-operation and Development: Paris, 1997.
(31) Panak, P. J.; Geist, A. *Chem. Rev.* **2013**, *113*, 1199.
(32) Allen, P. G.; Bucher, J. J.; Shuh, D. K.; Edelstein, N. M.; Craig, I. *Inorg. Chem.* **2000**, *39*, 595.
(33) Shannon, R. D. *Acta Crystallogr., A* **1976**, *32*, 751.
(34) Dalba, G.; Fornasini, P. *J. Synchrotron Radiat.* **1997**, *4*, 243.